

To be submitted to Nuovo Cimento A

LNF-91/021 (P)
6 Maggio 1991

D. Babusci, M. Castellano, N. Cavallo, F. Cevenini, A. Ghigo:

**LASER DIAGNOSTICS OF HIGH POWER LOW ENERGY ELECTRON
BEAMS**

LASER DIAGNOSTICS OF HIGH POWER LOW ENERGY ELECTRON BEAMS

D.Babusci, M.Castellano, A.Ghigo
INFN, Laboratori Nazionali di Frascati, P.O. Box 13, 00044 FRASCATI (RM) ITALY

N.Cavallo and F.Cevenini
INFN-Sezione di Napoli and Dip. di Scienze Fisiche dell'Universita' di Napoli, pad.19-20, Mostra d'Oltremare, I-80125 NAPOLI - ITALY

1. - INTRODUCTION

Dense and cold electron beams can be of extreme interest for ion beam cooling [1] and for the generation of coherent electromagnetic radiation in the microwave range through the Free Electron Laser process [2].

The high current needed in these applications requires a very efficient energy recovery in the electron accelerator, to save installed power, so that nondestructive diagnostics have to be taken into account for full intensity tests.

A project of a high-energy electron cooling device is actually in progress as an INFN collaboration. Several prototypes have been successfully tested and the final version has been constructed in the Frascati Laboratories. The first tests will be performed in the Legnaro Laboratories [3]. The apparatus consists of a high-frequency (40 kHz) Cockcroft-Walton generator (760 kV nominal voltage) with very low ripple (10^{-4}) and high stability, a Pierce electron gun followed by an accelerating tube and an energy recovery system. The energy recovery system consists of a decelerating column, similar to the accelerating one, and a collector. In order to compensate the space charge effects for all the operating energies, the electron beam is guided by an axial magnetic field.

A detailed description of the whole apparatus has been already published [3], while in Table I the main characteristics of the device are summarized.

The transverse beam temperature will be measured by means of a pair of synchronous wave pick-up matched to the electron cyclotron frequency [4], and positioned at the two ends of the straight section. The same instrument can also give the beam position, allowing the reconstruction of the electron line of flight. The longitudinal energy spread and the transverse beam density can be measured from the spectral width and relative intensity of a laser light backward scattered from the electron beam [5].

Table I - Characteristics of the electron cooling device.

Electron beam energy	(0.1 + 0.7)	MeV
Electron current	3.5	A
Electron beam diameter	3	cm
Electron momentum spread	10^{-3}	
Electron transverse temperature	1	eV
Collector voltage	(0.5 + 6)	kV
Magnetic field	3	kG
Drift region length	1.5	m

A feasibility study of this type of measurement on our gun has been already published [6], showing that, given an adequate laser power, a longitudinal momentum spread of the order of 10^{-4} can be measured.

In this paper we give a complete and detailed description of the whole experimental set-up. A Montecarlo code has been used to determine the geometrical and spectral properties of the scattered radiation. Using the Montecarlo results and the real characteristics of commercially available lasers, the more suitable measurement techniques and instrumentation have been defined, allowing us to obtain a precise evaluation of the energy range that can be covered and the ultimate achievable resolution.

2. - PHOTON SCATTERING FROM FREE ELECTRONS

The basic formalism of the photon scattering from free electrons and its use as a diagnostic tool in plasma and electron beam physics has been extensively reported [6], [7]. We will limit ourselves to a brief summary of the main features of the process which are fundamental to the technical choices of the experimental set-up.

The process, schematically shown in Fig. 1, is a backward Compton scattering, and the differential cross section, in the laboratory frame, is given by

$$d\sigma(\theta, \chi, \varphi) = \frac{r_0^2}{\gamma^4} \frac{1 + \beta \cos \theta}{(1 - \beta \cos \chi)^4} \{ (\beta - \cos \chi)^2 \gamma^2 + \sin^2 \varphi \sin^2 \chi \} d\Omega \quad (1)$$

with $d\Omega = \sin \chi \, d\chi \, d\varphi$, where β is the electron relativistic velocity factor, γ its energy in rest mass units, r_0 the classical electron radius, θ and χ the incident and scattered photon angles, respectively.

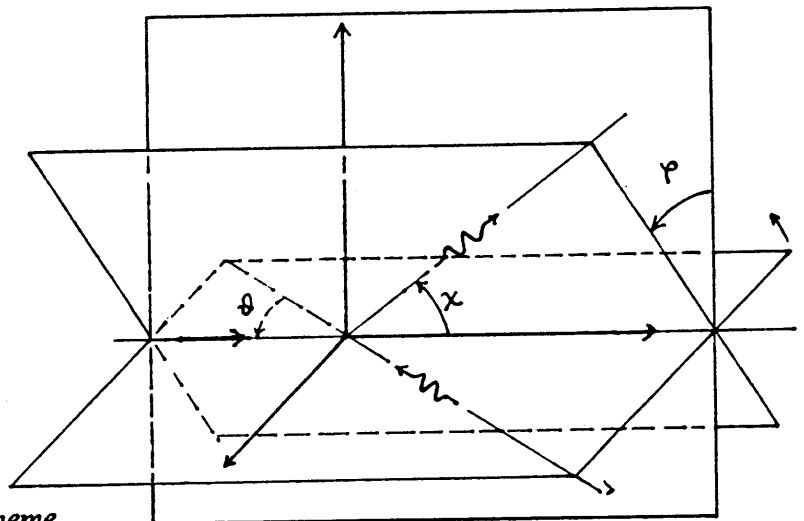


Fig. 1 Compton backscattering scheme.

Given the incident photon wavelength λ_0 , the scattered one is

$$\lambda_1 = \lambda_0 \frac{1 - \beta \cos \chi}{1 + \beta \cos \theta} \quad (2)$$

The differential scattering cross section is strongly peaked in the forward direction ($\chi=0$) so that we must measure the radiation in a small solid angle around this direction.

In order to assure the interaction between photons and electrons at the same radial coordinate along the whole straight section, the laser light must be parallel to the particle beam ($\theta=0$).

The broad electron energy range generates a scattered radiation spectral range which is too wide to be easily measured if a single frequency laser is used as light source. The use of two different laser beams (Nd at 1.06 μm and CO_2 at 10.6 μm) confines the radiation in the visible spectrum, where the measurement is much easier, in a relatively large energy range, as is shown in Fig. 2.

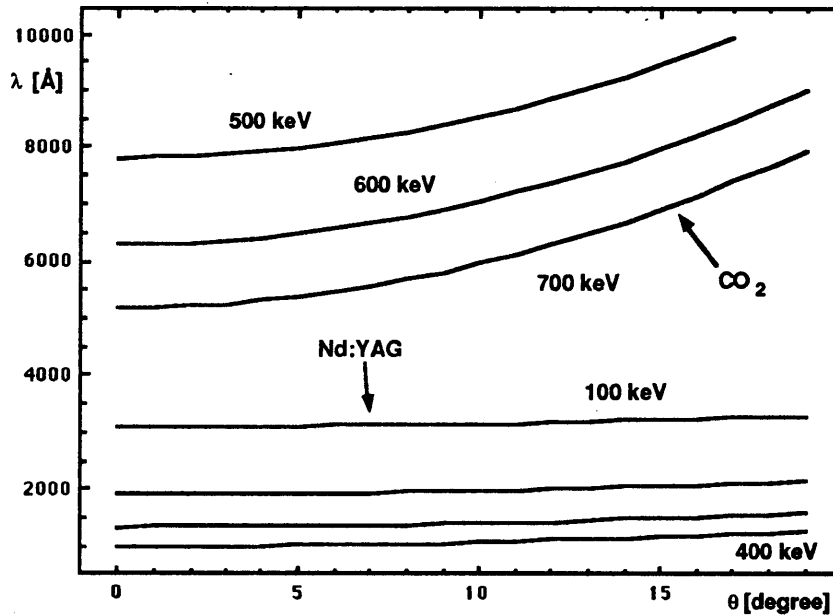


Fig. 2 - Scattered wavelength versus the radiation incident angle θ for different electron kinetic energy.

The low energy side, between 100 and 150 keV, which is of extreme interest at least in the first stage of the gun operation as a full current test of the energy recovery system, will be covered by a Nd-YAG laser.

The upper part of the energy range, between 500 and 700 keV, will be spanned by the 10.6 μm line of a CO_2 laser.

We can partially close the gap between these two ranges operating the same CO_2 laser at the 9.6 μm line, in this way going down to 400 keV, as can be seen in Fig. 3.

The scattered radiation wavelength is a function of the electron velocity and the scattering angle χ .

The measured line width is thus due to both the electron energy spread and the finite solid angle accepted by the measuring instrumentation.

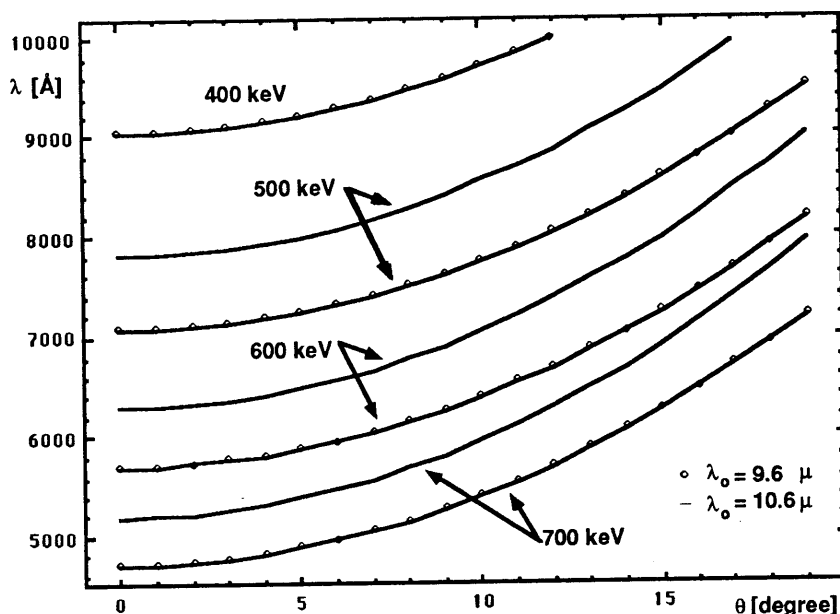


Fig. 3 - Scattered wavelength as Fig. 2 for different CO₂ lines.

An iris has to be placed along the scattered radiation path to reduce the accepted angle, and its aperture must be choiced to maximize the radiation intensity without affecting the energy spread measure resolution. This optimization is not straightforward, the radiation source being distributed along the whole straight section and the laser spot transverse dimension.

Moreover, a counting rate evaluation was necessary to define the measurement techniques and instrumentation, in order to evaluate the signal to noise ratio and thus the ultimate achievable resolution.

We decided to develop a Montecarlo computer code simulating the whole process and taking into account the real geometry to give an answer to all the forementioned questions.

3. - GENERAL LAYOUT

The accelerator machine we are dealing with is extensively described in reference 1 and 3.

The whole machine is placed in a restricted area that is suitable shielded by concrete walls due to the high beam power. This fact is mandatory because other experimental activities are hosted in the same building. The accelerator site as well as the shielding positions fixed the displacement of the main components of the measurement apparatus. Some of these, which necessarily have to be close to the straight section, have been installed inside the shielding walls and remote controlled. The laser device has been placed outside the walls in order to be easily operated and monitored.

The whole component layout has been arranged in order to have a very compact experimental area.

The measurements will be performed as follows. The laser radiation, focused in the centre of the straight section, interacts with the incoming electron beam. The backscattered radiation is splitted off from the laser and electron direction by a plane, 45° tilted, dichroic mirror and is focused into the monochromator.

A parallel displacement of the laser beam, respect to the trajectory main axis, allows the transverse scanning of the electron beam profile.

In order to do these measurements the main vacuum pipe is provided of two extensions that are aligned to the electron beam trajectory inside the 1.5 m straight section. The first of them, placed upstream respect to the electron motion, is closed by an optical window. The downstream extension consists of a chamber containing the dichroic mirror which is used to extract the backscattered radiation.

This chamber has two optical windows. The input infrared radiation passes through the first one, suitable centred, and interacts with the electron beam. The second window is perpendicular to the beam axis and allows the scattered radiation, which is reflected by the dichroic mirror, to be extracted. A high repeatability mechanical movement allows to keep the dichroic mirror away from the primary IR laser beam path.

The Montecarlo numerical simulation is used to evaluate the input laser power, the monochromator resolution, the dichroic mirror size as well as the photomultiplier and acquisition system performances. This simulation takes into account the constraints given by the aforementioned experimental apparatus and measurement.

4. - NUMERICAL SIMULATIONS

The goals of the numerical simulation were to study the frequency spectrum, the intensity of the backscattered radiation from the electron beam and the optimum collimator size.

The electrons were supposed uniformly distributed in a cylinder of 3 cm diameter and 150 cm length. The laser beam has a gaussian distribution on the transverse plane. The optical system is planned to realize a laser beam waist $w_0 = 5$ mm diameter located at the centre of the straight section. The transverse laser beam evolution in the interaction section is given by:

$$w = w_0 \sqrt{1 + \left[\frac{\lambda z}{\pi w_0^2} \right]^2}$$

where z is the longitudinal coordinate and λ the wavelength of the incident laser radiation.

There are two main approximation:

- a) the photon-electron interaction is head-on in all points of the straight section (the transverse temperature is < 1 eV);
- b) the contribution of the laser frequency width ($\Delta\lambda/\lambda < 10^{-5}$) to final spectrum is negligible respect to the electron beam energy spread.

The simulation main lines are:

- 1) the incident electron energy is extracted according to a gaussian distribution with mean value on the accelerator nominal energy and variance defined by the supposed longitudinal momentum spread;
- 2) the electron-photon longitudinal interaction point is extracted along the straight section according to the collision luminosity, with transverse coordinate distribution following the electron and photon beam convolution;
- 3) the scattered photon direction is extracted in the laboratory frame with cross section given by Klein-Nishina formula (1). The wavelength of the scattered photon is given by (2);
- 4) the scattered photons not passing through a filtering iris are rejected.

The first simulation series refer to the scattering of a CO₂ laser on a 700 keV electron beam.

The backscattered radiation linewidth produced by a momentum spread of 10^{-3} , which corresponds to the design value, with the photons selected by a large iris (20 cm diameter) is shown in Fig. 4. The distribution is very broad and clearly asymmetric so the determination of the electron energy spread is quite difficult.

The linewidth obtained by selecting the photons with a 5 cm diameter iris is shown in Fig. 5. The distribution is now symmetric and the gaussian fit (continuous line) gives a sigma value of 9.6 Å, to be compared with the theoretical one of 9.4 Å, i.e. a 2% accuracy in the momentum spread evaluation.

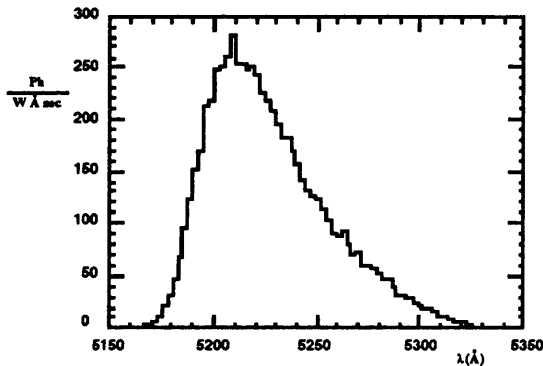


Fig. 4 - Spectrum of CO₂ backscattered photons flux through a $\Phi=20$ cm iris at 700 KeV and 10^{-3} momentum spread.

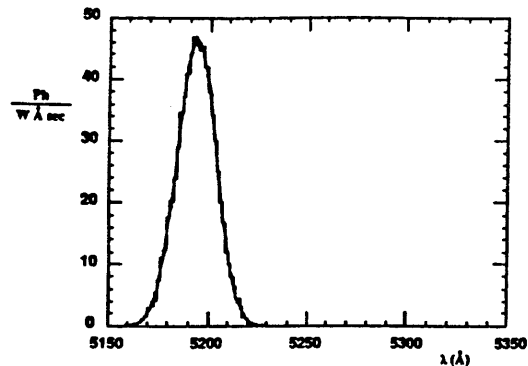


Fig. 5 - Spectrum of CO₂ backscattered photons flux through a $\Phi=5$ cm iris at 700 KeV and 10^{-3} momentum spread.

This iris dimension is determined by the size of the available mirror and real machine aperture, a 3 inches diameter mirror has been chosen. So that, taking into account the 45° tilt and the small screening of the mirror holder, the effective horizontal mirror acceptance is of the order of 5 cm. This means that we do not need a real iris, the mirror being itself the selecting element (for symmetry and practical reasons in the optical transport line we will also cut the radiation to the same size in the vertical dimension).

In these conditions the simulation gives a peak photons flux of 46 photons per second, with 1 W laser power and 1 Å optical linewidth.

If the electron momentum spread could be reduced to 10^{-4} the geometrical selection would not be sufficient, as shown in Fig. 6. In this case an iris with a diameter as low as 2 cm must be inserted to obtain an accurate momentum spread measurement, as shown in Fig. 7, from which we derive a photon flux of 12 photons/sec,W and 1 Å linewidth.

In the case of a Nd-YAG laser radiation on a 100 keV electron beam with a 10^{-3} momentum spread, the large scattering angle makes the iris completely unnecessary, as can be seen in Fig. 8, where the photon spectrum selected by a 20 cm iris is shown. No geometrical line widening is visible, and the linewidth (sigma value) of 3.95 Å corresponds, within 10 %, to the theoretical one.

With the photon selection performed by the dichroic mirror (equivalent to a 5 cm iris), the linewidth, as shown in Fig. 9, results equal to the theoretical one within 1 %. The same numerical simulation gives a maximum flux of 3.5 photons/sec,W and 1 Å linewidth.

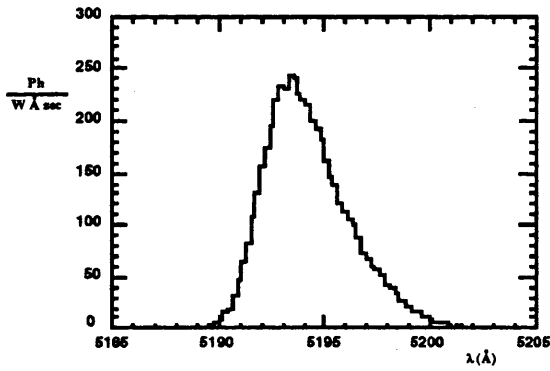


Fig. 6 - Spectrum of CO₂ backscattered photons flux through a $\Phi=5$ cm iris at 700 KeV and 10^{-4} momentum spread.

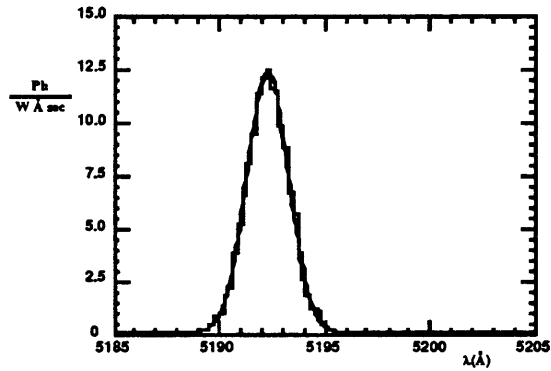


Fig. 7 - Spectrum of CO₂ backscattered photons flux through a $\Phi=2$ cm iris at 700 KeV and 10^{-4} momentum spread.

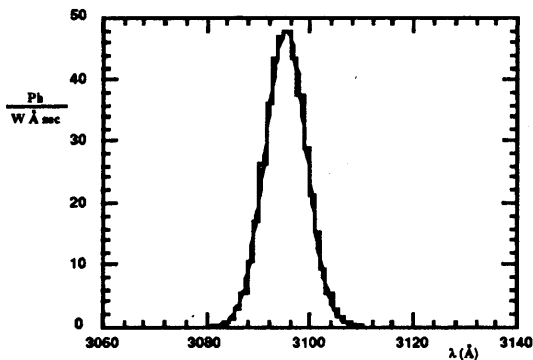


Fig. 8 - Spectrum of Nd-YAG backscattered photons flux through a $\Phi=20$ cm iris at 100 KeV and 10^{-3} momentum spread.

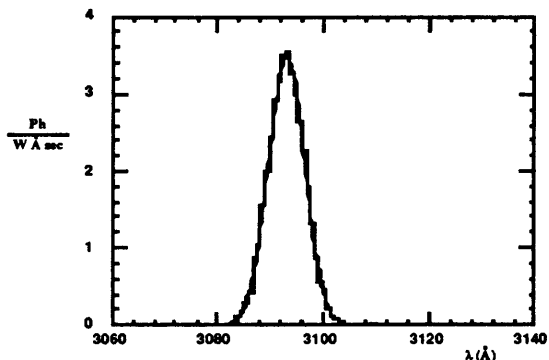


Fig. 9 - Spectrum of Nd-YAG backscattered photons flux through a $\Phi=5$ cm iris at 100 KeV and 10^{-3} momentum spread.

It is thus clear that in this case the main problem is the low value of the photon flux which can be obtained in real experimental conditions.

With an electron momentum spread of 10^{-4} we obtain the photon wavelength distribution shown in Fig. 10, the gaussian fit giving a sigma value of 0.36 \AA and a maximum flux of 32 photons/sec, W and 1 \AA linewidth.

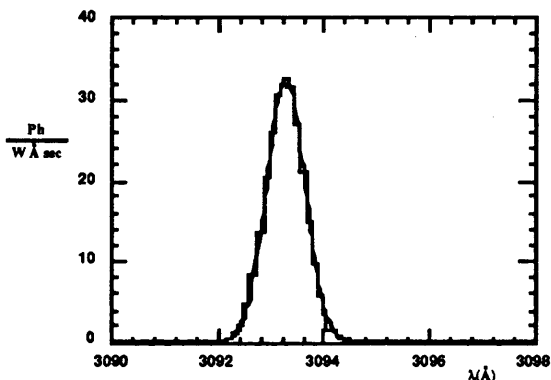


Fig. 10 - Spectrum of Nd-YAG backscattered photons flux through a $\Phi=5$ cm iris at 100 KeV and 10^{-4} momentum spread.

5. - LONGITUDINAL MOMENTUM SPREAD

5.1 - Experimental set-up

The proposed measurement of the momentum spread will be carried out as in the general scheme of Fig. 11 where the main components are shown.

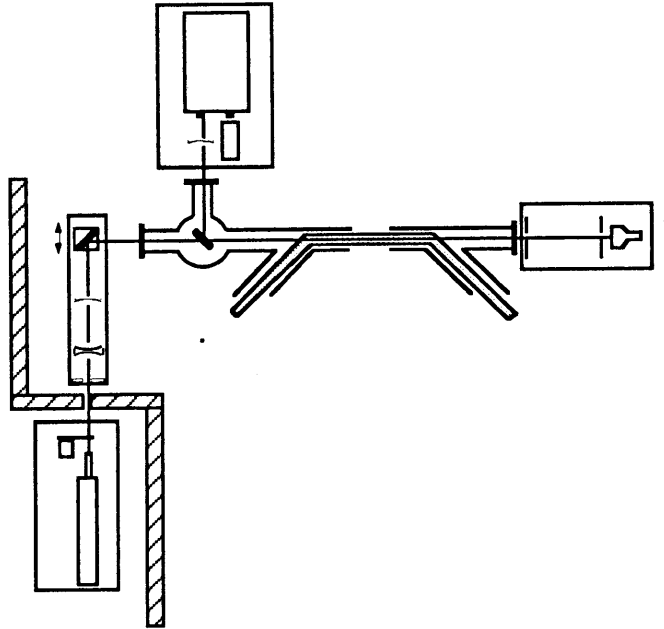


Fig. 11 - Experimental set-up

The laser beam is displaced at the electron beam level by means of a beam steering. Then it passes through an iris and an optical telescope which adjusts the input radiation envelope in order to have the appropriate waist in the centre of the interaction straight section. A movable 45° tilted mirror is used to scan the laser beam across the transverse profile of the electron one. The remote controlled displacement has been made perpendicular to the radiation axis.

After the interaction straight section, the laser beam pass through an iris and is absorbed by a radiation detector which is used for radiation intensity monitoring during the measurements.

The backscattered radiation is analysed by an optical system consisting of a lens, focusing the light on the input slits of a monochromator, the monochromator itself and a photomultiplier detector. The wavelength tuning is remote controlled. All the components are placed on suitable optical benches.

5.2 - Alignment procedures

The alignment procedure must cope with two problems: the difficulty of aligning a non visible IR laser on the vacuum pipe, which is considered a reference for the electron beam, by means of irises, and the low intensity of the backscattered radiation, on which the monochromator must be aligned.

To overcome these problems, a visible He-Ne laser is centred on the vacuum pipe, using the windows as reference and with the dichroic mirror removed from the beam line. The two previously mentioned irises, before and after the interaction region, are aligned on this laser beam.

The He-Ne laser is then moved on the output bench and backward directed, its beam centred on the two irises. Inserting the dichroic mirror, which reflects the red light of the laser, the monochromator and its related optics can be easily aligned.

The final step consists in aligning the IR laser beam through the two irises, after the removing of the He-Ne laser.

The distance between the two irises is about 5 m, so that, assuming a rather rough accuracy of 0.5 mm in the irises positioning, we obtain a 0.1 mrad accuracy in the laser alignment, which can be accepted by the monochromator.

A possible misalignment of the electron beam with respect to the vacuum pipe can be easily detected by the RF pick-ups and the laser direction corrected.

The photomultiplier will be placed on a remote controlled mounting so to optimise the position relative to the monochromator by maximizing the output signal.

5.3 - Low energy (100 keV) electron beam measurement

The low photon flux indicated by the numerical simulation in this energy range suggests the use of a photon counting technique to evaluate the backscattered radiation linewidth.

We will describe in this paragraph how this technique is implemented and the results that can be obtained.

A pulsed Nd:YAG Quantel YG 585/50 laser will be used for this measurement. The energy per pulse is about 280 mJ with 50 Hz repetition frequency. Other characteristic are shown in Table II.

Table II - Characteristics of the laser sources

	pulsed Nd:YAG (QUANTEL YG585-50)	CO ₂ c.w. (EDINBURGH PL5)
Wavelength	1.06 μm	9.6-10.6 μm
Energy per pulse	280 mJ	
Pulse duration	10-12 nsec	
Repetition frequency	50 Hz	
Average power	14 W	50 W
beam diameter	7 mm	7.5 mm
Divergence	0.7 mrad	<2 mrad
Amplitude stability	2.5% max	1% max
Frequency stability		2 MHz
	Quasi gaussian beam prof.	Gaussian beam profile

A ~ 4 % reflectivity beam splitter is placed just in front of the Nd:YAG laser on the same optical table and a very fast photodiode is used for the acquisition system timing. The alignment iris will be open accordingly to the laser beam size. The telescope lenses as well as the input and output windows of the vacuum pipe are BK7 made and A.R./A.R. coated at the 1.06 μm laser wavelength.

For the photon acceptance, as discussed in the previous paragraph, the effective aperture of the window has to be of the same order of the dichroic mirror size. To satisfy this requirement the optical glasses of the window have a 75 mm diameter; in this way its mounting on the

vacuum flange reduces the optical aperture to a bit more than 50 mm.

The dichroic mirror is coated in order to have the maximum transmissivity at 1.06 μm as well as the maximum reflectivity between 295 and 325 nm, because the backscattered radiation is Doppler-shifted at about 310 nm. The herasil output window has an effective diameter of 50 mm and it is A.R./A.R. coated in order to have the flat transmissivity between 300 and 700 nm.

The Jobin Yvon HRS-2 monochromator can be operated at maximum resolution of 0.2 \AA with a 1200 grooves/mm grating blazed at 330 nm. A Thorn-EMI 9893-QB/350 photomultiplier with high gain ($\sim 8 \times 10^7$ typical) and very low dark current (150 cps maximum in between -30°C and 60°C of temperature) will be used as radiation detector. It is provided of a cooled housing with a temperature range of $+15^\circ\text{C}$ to -25°C , controllable within 0.1°C . The effective photocathode dimension (~ 9 mm of diameter) demands a careful optimization of the detector position; this suggests the movement remotization, as stated in the previous paragraph.

To determine the photon counting rate we start from the Montecarlo result of Fig. 4, i.e. for an electron momentum spread of 10^{-3} and the dichroic mirror as geometrical selecting element. The photon flux hitting the photomultiplier cathode is reduced by the losses introduced by the optical elements: lenses, mirrors, monochromator etc. The photoelectron number, which gives the final counting rate, depends on the quantum efficiency of the cathode itself.

If we scan the linewidth with a monochromator resolution of 1 \AA , taking into account the laser power of 14 W, the overall optical losses evaluated of the order of 31 %, and the photomultiplier cathode quantum efficiency of 20 %, we obtain a peak counting rate of 6.6 counts/second, corresponding, for the laser frequency of 50 pulses/second, to 0.13 counts/pulse.

This counting rate confirms the possibility of using a photon counting technique. In fact the probability of a double photon event is as low as 0.8 %, while the photomultiplier background counting can be kept at the level of 2.5×10^{-3} counts/pulse by the use of a 50 ns gate on the counting unit. The background due to the cathode blackbody radiation and to the electron bremsstrahlung on the residual gas is estimated to be even lower.

The acquisition system is shown in Fig.12.

If the electron energy spread results larger than the design value, the same total number of photons per second will be collected, the intensity being determined only by the beam energy and geometrical acceptance, but distributed on a wider spectral line.

We can keep constant the experimental counting rate simply proportionally increasing the output bandwidth of the monochromator, that is measuring the linewidth with the same number of experimental points.

In these conditions we are able to fully reconstruct the optical line with 15 measurements ($\pm 2 \sigma$) of 1.5 minutes each, obtaining an accuracy, due to statistical error only, of 4% on the peak, and of 5.2% at one σ . It is thus possible to achieve a good measure of the electron beam energy spread in a little more than 20 minutes. During measuring time both the laser and electron beam intensities will be monitored in order to normalize the experimental results.

On the other hand, if the energy spread happens to be of the order of 10^{-4} , the monochromator must be pushed to its ultimate resolution to resolve the backscattered radiation line, but the hypothesis of a negligible laser linewidth would not be more valid. Although one could be satisfied by reaching such a low energy spread, it is possible to measure it with a different experimental arrangement.

An intracavity etalon can reduce the laser linewidth, at the price of a reduced output

power, and, if necessary, a Fabry-Perot interferometer can be used for wavelength selection of the scattered radiation.

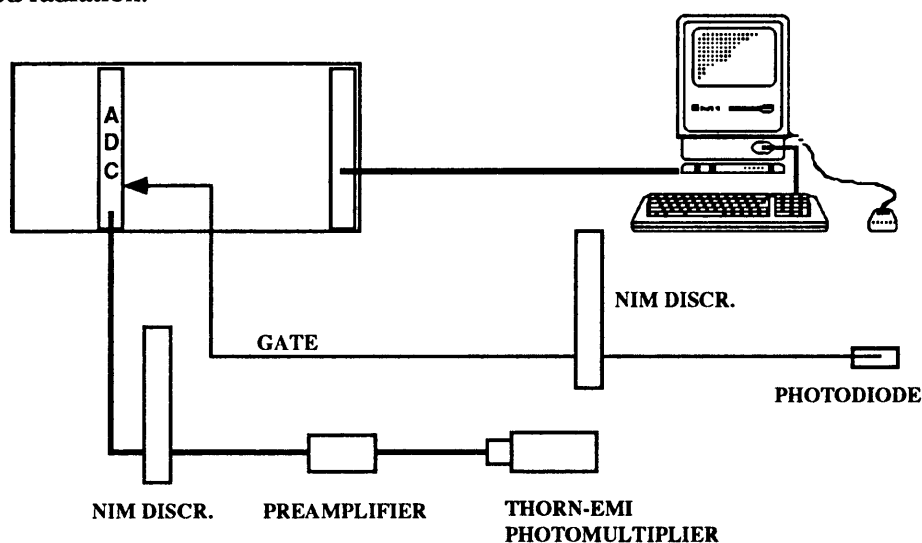


Fig. 12 - Schematic layout of the acquisition system for the low energy measurement.

5.4 - High energy (450-700 keV) electron beam measurement

For the high energy measurement, a c.w. CO₂ laser (Edinburgh Instruments PL5) is utilized, delivering over 50 W output power on the single line.

The extracavity PL5-SF spatial filter cuts higher laser modes and an opto-galvanic stabilizer provides a long term frequency stability of the order of 2 MHz.

In order to match the whole optical system to the CO₂ wavelength, the optical elements have to be changed respect to the low energy measurements. In particular both the windows at the end of the vacuum chamber will be made of ZnSe with 10.6 μm A.R./A.R. coating.

The Germanium dichroic mirror has maximum transmissivity at the same wavelength and maximum reflectivity centered in the visible region because the backscattered radiation covers the spectral range between 780 and 520 nm, corresponding to 500 and 700 keV electron kinetic energies. Also the monochromator grating must be changed with a 750 nm blazed one.

For the 9.6 μm line, the backscattered wavelength will be a bit lower (of the order of 700 and 470 nm for 500 and 700 keV electron energies), but all the following discussion remains valid.

The peak flux given by the Montecarlo calculation, as shown in Fig. 5, suggests us to use a different measuring technique.

The use of a high power CW laser can be best exploited by a synchronous demodulation of the laser signal, mechanically chopped, by a lock-in amplifier. For this purpose a EG&G 5206 Lock-in amplifier is used for the signal detected by the RCA C31034 photomultiplier. The laser intensity after the interaction region is continuously monitored. The acquisition system is shown in Fig. 13.

The relatively low gain of the photomultiplier (4.8×10^5 typical), which is preferred for its flat response in the range of 300-900 nm wavelength, is compensated by the high gain of the KEITHLEY 428 current amplifier ($10^3 \div 10^{11}$ V/A).

Starting from the 50 W laser power, taking into account the 50% transmission efficiency of

the chopper, the total optical losses of 34%, and the photomultiplier quantum efficiency of 20%, we achieve, in the case of an electron momentum spread of 10^{-3} , a final peak counting rate of 153 pulses/second with a monochromator resolution of 1 Å.

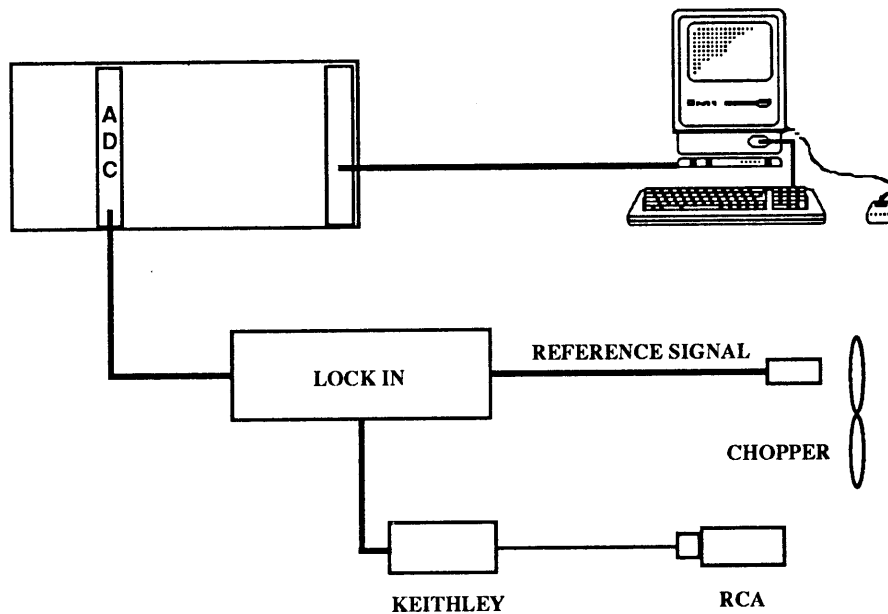


Fig. 13 - Schematic layout of the acquisition system for the high energy measurement.

The linewidth of the backscattered radiation allows us to use a measuring resolution of 2 Å, obtaining a maximum counting rate of 306 pulses/second, which corresponds to a mean current of 24 pA from the photomultiplier. With an easily manageable current to voltage gain of 10^9 we obtain 24 mV to the lock-in amplifier input.

A few seconds lock-in integrating time is thus enough to reach the desired measuring accuracy. The high selectivity of the demodulation technique makes the background completely negligible.

The whole line will be analyzed in a few minutes, allowing also the scanning of different beam position in the horizontal plane during the same accelerator run, without worry of change in parameter settings.

The same arguments discussed for the low energy measurement remains valid in the case of larger energy spread.

On the contrary, if an energy spread as low as 10^{-4} can be reached, the same experimental set-up will permit an accurate linewidth measurement, due to the very narrow laser bandwidth and the larger photon spectrum. The reduced photon flux can be easily coped by an increase of the current to voltage gain and a longer lock-in integrating time.

6. - CONCLUSIONS

We have shown that an accurate electron energy distribution measurement can be performed in a nondestructive way, allowing an efficient electron energy recovery. Using commercial instrumentation it is possible to measure an energy spread of less than 10^{-3} in two different energy regions: around 100 keV and from 450 to 700 keV.

All the instruments described in the paper have been already acquired and tested, and the measurements will be performed soon after the first tests of the accelerator.

The only difficulty can arise from an energy recovery less efficient than the design goal. In fact we estimate that at least a 1 A current is needed in the low energy case to obtain a tolerable counting rate.

In the high energy case a lower current can be accepted, due to the higher power of the laser and to the much more collimated backscattered radiation, but at least few hundreds mA are required.

REFERENCE

- [1] U.Bizzarri, M.Conte, R.Scrimaglio, L.Tecchio and A.Vignati: *High-Energy Electron Cooling at LEAR*, Nuovo Cimento A, **73**, 425 (1983);
- [2] I.Boscolo, G.Brautti, V.Stagno, L.Tecchio and V.Variale: *A CW high power and high quality electrostatic accelerator for FEL devices*, Proc. of 'European Particle Accelerator Conference' Rome, 1988, S.Tazzari Ed., World Scientific Publ. Co. 1989;
- [3] R.Calabrese, F.Petrucci, M.Savriè and L.Tecchio: *Design of the Beam Line and Energy Recovery System for High-Energy Electron Cooling Device* Nuovo Cimento A, **100**, 763 (1988);
- [4] G.Di Massa, M.R.Masullo, V.G.Vaccaro, V.Lollo, R.Calabrese, F.Petrucci, L.Tecchio: *Transversal temperature measurement in electron cooling experiment*, Nuovo Cimento A, **102**, 823 (1989);
- [5] B.Kells: *Laser diagnostic for electron cooling beam*, Fermilab Rep. TM-771 1503.000, (1978);
C.Habfast, H.Poth, B.Seligmann, A.Wolf, J.Berger, P.Blatt, P.Hauck, W.Meyer and R.Neumann: *Measurement of laser light Thomson-scattered from a cooling electron beam*, CERN-EP/87-71,1987
- [6] L.Tecchio, C.Salvetti, L.Busso, F.Tosello, R.Calabrese, F.Petrucci, M.Savriè, M.Conte and G.Simone: *Diagnostics with a Laser Beam in Electron Cooling Experiment*, Nuovo Cimento B, **85**, 217 (1985);
- [7] U.Schumacher: *Electron ring diagnostic with light scattering*, Max-Plank Institute fur Plasmaphysik, IPP 0/36 (1977)